

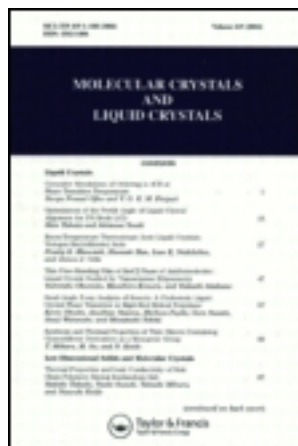
This article was downloaded by: [Tomsk State University of Control Systems and Radio]

On: 19 February 2013, At: 12:11

Publisher: Taylor & Francis

Informa Ltd Registered in England and Wales Registered Number: 1072954

Registered office: Mortimer House, 37-41 Mortimer Street, London W1T 3JH, UK



## Molecular Crystals and Liquid Crystals Incorporating Nonlinear Optics

Publication details, including instructions for authors and subscription information:

<http://www.tandfonline.com/loi/gmcl17>

## Rheology, Phase Equilibria and Processing of Lyotropic Liquid Crystalline Polymers

V. G. Kulichikhin<sup>a</sup>

<sup>a</sup> Institute of Petrochemical Synthesis, USSR Academy of Sciences, 117912, Moscow, USSR

Version of record first published: 03 Jan 2007.

To cite this article: V. G. Kulichikhin (1989): Rheology, Phase Equilibria and Processing of Lyotropic Liquid Crystalline Polymers, *Molecular Crystals and Liquid Crystals Incorporating Nonlinear Optics*, 169:1, 51-81

To link to this article: <http://dx.doi.org/10.1080/00268948908062733>

PLEASE SCROLL DOWN FOR ARTICLE

Full terms and conditions of use: <http://www.tandfonline.com/page/terms-and-conditions>

This article may be used for research, teaching, and private study purposes. Any substantial or systematic reproduction, redistribution, reselling, loan, sub-licensing, systematic supply, or distribution in any form to anyone is expressly forbidden.

The publisher does not give any warranty express or implied or make any representation that the contents will be complete or accurate or up to date. The accuracy of any instructions, formulae, and drug doses should be independently verified with primary sources. The publisher shall not be liable for any loss, actions, claims, proceedings, demand, or costs or damages whatsoever or howsoever caused arising directly or indirectly in connection with or arising out of the use of this material.

# Rheology, Phase Equilibria and Processing of Lyotropic Liquid Crystalline Polymers

V. G. KULICHIKHIN

*Institute of Petrochemical Synthesis, USSR Academy of Sciences, 117912 Moscow, USSR*

The structure and rheological properties of liquid-crystalline solutions of stiff-chain and semi-stiff-chain polymers are analyzed in connection with the peculiarities of their phase states. Of special importance are the observation and reasonable utilization of optimal thermodynamic conditions in combination with rheological properties in processing lyotropic polymers.

*Keywords: rheology, processing, lyotropic polymer, phase equilibria*

The liquid crystalline (LC) state is a thermodynamic equilibrium phase state which is characterized by a stable anisotropic structure and properties resulting from a one-dimensional or two-dimensional ordering. Strange as it is, in spite of the fact that polymer molecules are, in general, asymmetric, the LC-state was first recorded in solutions, not in melts. This may be explained by the fact that at that time it was necessary to process stiff-chain polymers in solutions as their melting point is, as a rule, higher than the decomposition point. Earlier, science and technology were not familiar with semi-stiff-chain polymers containing mesogenic groups in the main or side chains. Besides, the concept of "mesogenic groups" in the polymer chemistry did not receive widespread attention. Later on, however, such polymers comprised a new class of thermotropic LC-polymers which are considered in this special issue.

Depending on the method of conversion of the system into a LC-state, we may distinguish two types of LC polymer systems: thermotropic and lyotropic. The LC-phase in the former system is formed by varying the temperature of individual substances; the latter by adding a low-molecular solvent. The solution, in its turn, can undergo mesophase transitions over a temperature scale; thermotropic polymers were also reported to form a LC-phase in solution. The literature available on low-molecular liquid crystals refer lyotropic LC to those LC-systems in which mesophases are formed only in the presence of a solvent (amphiphilic systems, phospholipid membranes, etc.). With respect to polymers, the concept of lyotropic liquid crystals was extended to solutions. No such behavior has been observed among low-molecular LC analogs, although the widely used mixtures of nematic substances in that compositional region where they are indefinitely compatible, can also be ascribed to anisotropic solution.

Thermodynamic conditionality of LC-state, its lability, and consequently, its fluidity are inherent characteristics of LC-systems. Of special importance are the observation and reasonable utilization of optimal thermodynamic conditions in combination with rheological properties in processing LC-melts and solutions. Such problems will be discussed in the present review.

## PHASE EQUILIBRIA IN STIFF-CHAIN POLYMER SOLUTIONS

Possible phase states for solutions are described by the combination of the concentration  $C$  with the Flory-Huggins parameter interaction (or temperature,  $T$ ), i.e., by means of the phase diagrams. Theoretically, the transition of solutions of stiff- and semi-stiff-chains to a LC-state is predicted, as a general rule, by the statistical thermodynamic theory involving virial<sup>1</sup> or lattice models<sup>2</sup> and the parameter describing the degree of disorientation of the macromolecules. The results of the analysis of the change in the free energy of the system have shown that when the degree of filling of the athermic solution with stiff macromolecules is enhanced, there appears a moment when it is impossible to maintain the disordered distribution of the system of chains available without changing its stiffness (when a new macromolecule is introduced). A further increase in the solution concentration is thermodynamically beneficial, provided an ordered packing of the macromolecules or realization of the nonequilibrium conformations is ensured.

The general view of the theoretical phase diagram for a rods-solvent system is presented in Figure 1 (according to Reference 2). For solutions with temperature  $T_0$ , the appearance of an anisotropic (LC) phase in the system is a result of concentration  $C^*$ . The mixture of isotropic (I) and LC-phase, narrow at high  $T$  and broad at low  $T$  values, is typical of this diagram.

The experimental investigation of the phase states in stiff-chain polymer solutions provides evidence for a close correlation in the true and theoretical diagrams only for a solution of helix polypeptides.<sup>3</sup> At the present time, the center of gravity of

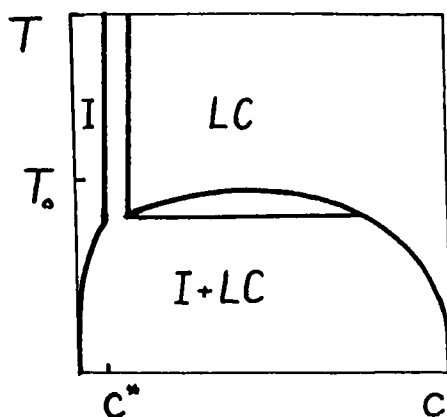


FIGURE 1 The theoretical phase diagram according to Flory.<sup>2</sup>

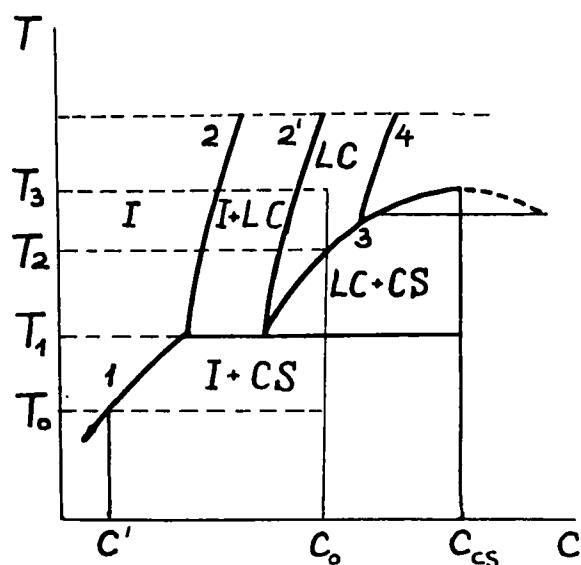


FIGURE 2 A schematic presentation of the phase diagram for *p*-linked aromatic polyamide-sulfuric acid systems<sup>9,10</sup> (see explanation in the text).

experimental investigations holds for the thermotropic systems. The content of this special issue is a witness to this fact. However, the theoretical papers describing the phase equilibria in solutions from the position of statistical physics continue to appear on the scene and refine the initial theoretical proposition concerning semi-stiff chains,<sup>4</sup> macromolecules with different flexibility mechanism (including persistent, free-joined and rotation-isomeric),<sup>5,6</sup> mixtures of stiff rods of diverse lengths, etc.

The theories available do not take into account such a strong solvent-polymer interaction which leads to the existence of crystal-solvates (CS). Such a solid phase is formed in solutions of aromatic polyamides of *p*-structure in mineral acids, as a rule.<sup>8,9</sup> In crystalline lattice CS, elementary polymer links and solvent molecules enter simultaneously into definite mole ratios.

Let us consider the most important part of the phase diagram (Figure 2). As the temperature rises, the system containing concentration  $C_0$  passes through the following regions. In the case of  $T_0$ , it is a mixture containing isotropic solution with concentration  $C'$  and CS with composition  $C_{cs}$ . In that region the system acquires considerable fluidity. At  $T_2$ , there occurs a transition to a complete LC solution. For example, at temperature  $T_3$  and polymer concentration  $C_0$  the system contains no other phase, except the liquid-crystalline.

Thus, the phase diagram for aromatic polyamide solutions in acids describes the equilibria: I-CS, LC-CS and I-LC. The variant of the phase diagram presented in Figure 2 considers a case of incongruent melting of the crystal-solvate, the curve 4 separates the region where the phase equilibrium occurs between the anisotropic solution and crystalline polymer. It is quite possible, however, that one may observe in certain cases the formation of CS with a higher mole ratio of polymer to solvent.

## RHEOLOGICAL PROPERTIES OF ISOTROPIC STIFF-CHAIN POLYMER SOLUTIONS

Different regions of the phase diagram respond to definite rheological properties of solutions conditioned by the peculiarities of a particular phase. Let us analyze those properties starting with the extreme left end of the diagram region, i.e., the isotropic solution region. With respect to the isotropic low-molecular and polymer systems, it should be emphasized that both systems are distinguished from each other in that the former is of a Newtonian fluid, the latter reveals appreciable non-linear effects. Therefore a closer rheological analog of the isotropic solution of stiff-chain mesophasogenic polymers will be the corresponding flexible-chain polymer solutions but not the low-molecular LC at a temperature above clearing point.

In a general case, the concentration dependence of viscosity of the polymer solutions allows one to construct a single curve using the modified Martin equation coordinates.<sup>6,11</sup>

$$\eta_i = C[\eta] \exp K_M C[\eta] (C/C_c)^\beta$$

where  $\eta_i$  is the relative viscosity increment;  $K_M$ , the Martin constant;  $C_c$ , the concentration corresponding to the onset of interpenetration of the molecular coils;  $\beta$ , the degree index in the formula  $\eta \sim C^\beta$ . The factor  $(C/C_c)^\beta$  appears only for concentrated solutions and takes account of the increase in the density of the interchain contacts with increasing concentration, whereas for dilute solutions, the Martin equation functions in the traditional manner.

Such a generalized dependence of viscosity for a series of polymers with different stiffness of macromolecules (the Kuhn's segment lengths range from 15 to 500 Å) is presented in Figure 3. The LC-solution region is temporarily excluded from consideration. This is purposely done in order to analyze the parameters determining the viscosity and their variation with macromolecule stiffness, from typically flexible chain polymer to a mesophase polymer.

Although in a general case the rheological properties of isotropic solutions of the flexible-chain and stiff-chain polymers are of one type in terms of absolute values of such parameters as  $K_M$ ,  $[\eta]$ ,  $C_c$  and  $\beta$ , one may observe the specificity of the behavior of solutions of stiff chains.<sup>12</sup> Thus, the value  $[\eta]$  corresponding to the hydrodynamic macromolecule volume is always higher for the rigid-chain polymers. The value  $K_M$  usually rises with increasing macromolecule stiffness, whereas  $\beta$  can behave in a more complicated fashion and vary depending on the concentration interval ( $C_c - C^*$ ) ranging from 3 to 6 (see below). At the same time, the value  $\alpha$  in the formula  $\eta \sim M^\alpha$  reaches 6–8 (see Reference 13). All this leads to a higher value of the initial viscosity of the isotropic solutions of the stiff-chain polymers in comparison with the equiconcentrated solutions of the flexible-chain polymers.

As for initial viscosity, we are dealing with practically a non-destructable macromolecular structure. If the structure is destroyed due to deformation, there may occur new effects whose scale will differ for flexible and stiff chains, respectively.

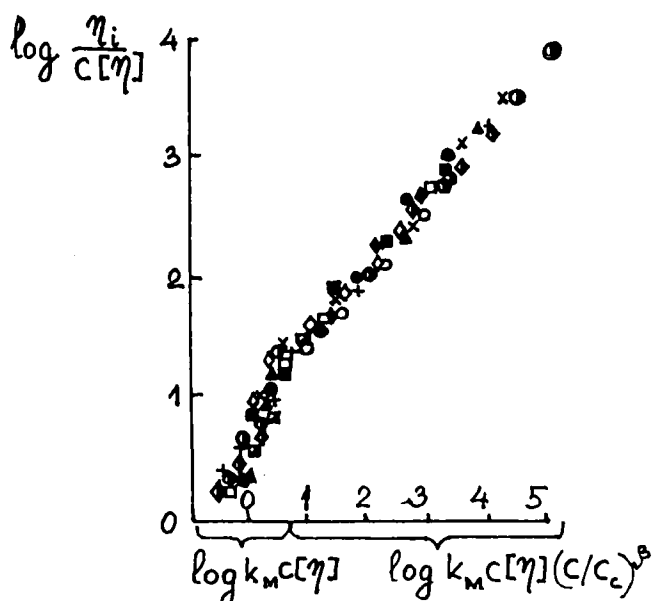


FIGURE 3 Generalized dependence of polymer solution viscosity on concentration. Different points correspond to different polymers among which the most flexible-chain is the polycapraamide, and the most stiff-chain is the poly-*p*-benzamide (according to References 11 and 12).

Thus, the dependence of viscosity on the intensity of deformation (shear rate  $\dot{\gamma}$  or shear stress  $\tau$ ) is essential for viscoelastic polymer systems. Such dependences for poly-*p*-phenyleneterephthalamide (PPTA) and polyamide 6,6 in concentrated sulfuric acid under conditions similar to C and M are presented in Figure 4 (according to Reference 14). The solution viscosity of the stiff-chain polymer in the region of low  $\tau$  is substantially higher. However, with a rising shear rate the difference starts to decline at the expense of a sharper decrease in the PPTA solution viscosity. This may be the result of the influence of two factors: destruction of a denser intermolecular contact system and the increasing role of the orientation processes in the stream. The orientation is most pronounced in dilute stiff-chain polymer solutions (a substantial decrease in the disorientation angle of stiff molecules in a shear flow can be achieved for dilute biopolymer solutions at high rates).<sup>15</sup> The orientation effects lead to a decrease in the internal friction coefficient.

## RHEOLOGICAL PROPERTIES OF LC POLYMER SOLUTIONS

From what has been cited above, it is clear that there appears and accumulates such a peculiarity in the isotropic stiff-chain polymer solutions which in the LC-state becomes the determining factor in the rheological properties of these systems. This peculiarity consists of the anisotropic viscoelastic characteristics, i.e., their dependences on the reciprocal positions of the long molecule axis, shear movement and shear rate directions. The concept of viscosity anisotropy is widely spread in

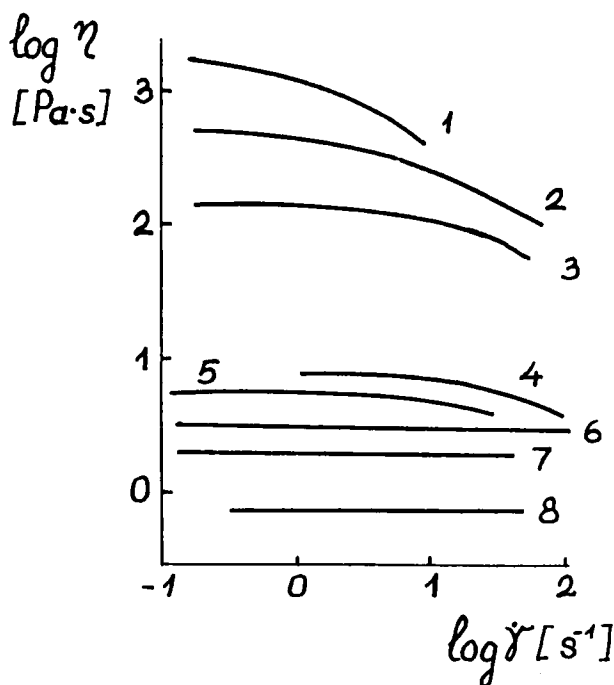


FIGURE 4 The dependence of viscosity on the shear stress for equi-concentrated sulfuric acid solutions of nylon 6,6 (1–4) and PPTA (5–8); molecular weights  $3.2 \times 10^4$  (1),  $2.76 \times 10^4$  (2),  $2.02 \times 10^4$  (3),  $1.28 \times 10^4$  (4),  $4.23 \times 10^4$  (5),  $3.52 \times 10^4$  (6),  $2.51 \times 10^4$  (7),  $1.45 \times 10^4$  (8).

low molecular liquid crystal physics, since the local rheological situation for them is essential for predicting the orientation and reorientation effects caused by the electromagnetic field in optoelectronic devices. The problem of determining the averaged rheological characteristics is most important for polymer systems. Such characteristics are available in processing them in materials (fibers, films, etc.). Nevertheless, the knowledge of anisotropic viscosity and elasticity coefficients is, without doubt, useful both for formulating constitutive rheological equations and for predicting and explaining the experimental effects even in uncontrollable orientations, typical of ordinary rheological polymer experiments.

The present paper does not deal in detail with theoretical problems, but it should be emphasized that, as distinct from the approaches usually used in describing the dynamics of low-molecular nematogens based on the Ericksen-Leslie theories,<sup>16</sup> it is reasonable to introduce a time derivative stress when conducting phenomenological analysis of the rheology of polymer systems. In other words, instead of the Newton law for linear-viscous anisotropic fluid describing the relation between the stress field  $\sigma_{ik}$  and shear rate field  $\dot{\gamma}_{ln}$ :

$$\sigma_{ik} = P_{ih} + \eta_{ikln} \cdot \dot{\gamma}_{ln}$$

where  $P_{ik}$  is the equilibrium stress,  $\eta_{ikln}$  is the viscosity tensor, one should apply the visco-elastic fluid equation with memory:

$$\theta_{ikln} \frac{\Delta \sigma_{kl}^1}{\Delta t} + \sigma_{ij}^1 = \eta_{ikln} \cdot \dot{\gamma}_{ln}.$$

The addition of a member containing an invariant time derivative from the stress tensor enables one to describe the anisotropic stress relaxation characteristic of LC-polymers.

### Viscosity anisotropy of LC-polymer systems

The measurements of the anisotropic viscous characteristics need special techniques in order to develop, maintain and control the molecular orientation during the experiment. The magnetic field is most often used for the orientation. The experimental data on viscosity anisotropy in LC-polymers are practically absent. Some indirect considerations concerning the influence of the initial texture of the LC-system, operation unit geometry, molecular orientation in the wall layer on the rheological characteristics being measured are presented in References 18 and 19. The use of ordinary rotational or capillary devices, due to the significant molecular orientation of the liquid crystals in the direction of the movement, renders it possible to measure viscosity values ( $\eta$ ). They are close to the least anisotropic viscosity Miesovitch coefficient.<sup>20</sup> However, a small modification of the operation unit of the cylinder-cylinder type permits estimating the anisotropic viscosity coefficients. The modification involves the utilization of the transparent outer cylinder, which renders it possible to record the duration of a hard ball falling in the clearance under conditions of a shear of the anisotropic material. The anisotropy of the medium complicates slightly the ordinary calculation of viscosity as the law of resistance is unknown for a testing ball. It has been shown that the resistance force acting on the ball  $F_i$  depends on the direction of its movement, i.e., there occurs a mobility anisotropy of the body isotropic in shape. When the ball moves in parallel ( $\parallel$ ) or perpendicular ( $\perp$ ) to the director  $\mathbf{n}$ , the usual Stokes law of resistance is valid:

$$F_i^{\parallel} = -\zeta_{\parallel} u_i; \quad \zeta_{\parallel} = 6\pi d \eta_{\parallel};$$

$$F_i^{\perp} = -\zeta_{\perp} u_i; \quad \zeta_{\perp} = 6\pi d \eta_{\perp};$$

Here  $u_i$  is the linear rate of the ball,  $\zeta_{\parallel}$  and  $\zeta_{\perp}$  are the longitudinal and transverse resistance coefficients with respect to  $\mathbf{n}$ ;  $\eta_{\parallel}$  and  $\eta_{\perp}$  are the longitudinal and transverse viscosity coefficients,  $d$  is the ball's diameter.

If the ideal molecular orientation is attained in the clearance, the longitudinal and transverse viscosity coefficients would equal the corresponding Miesovitch viscosity coefficients. However, because it is practically impossible to achieve an



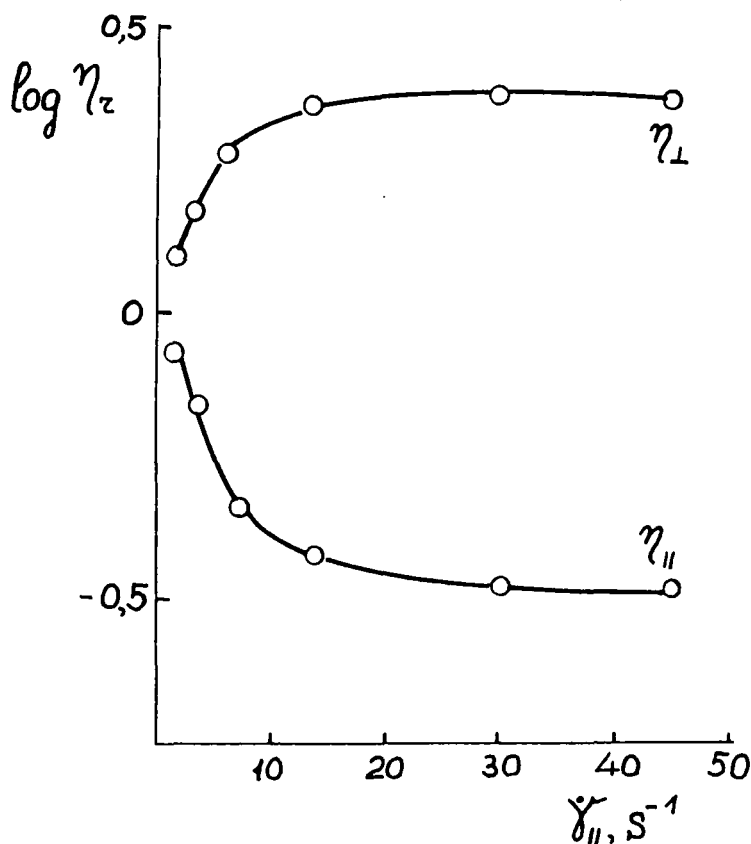


FIGURE 5 The dependence of the relative values  $\eta_{||}$  and  $\eta_z$  on  $\dot{\gamma}_{||}$  for LC-solutions of PBA in DMAA with 3% LiCl.

ideal orientation in the shear flow, such experiments point only to the presence of a viscosity anisotropy.

We shall not dwell on the details of these experiments, but only show by example of poly-*p*-benzamide (PBA) solution in dimethylacetamide with 3% LiCl the end results in Figure 5.<sup>6,21</sup> As the rate gradient  $\dot{\gamma}_{||}$  rises, the value  $\eta_{||}$  decreases, while  $\eta_z$  increases reaching at  $\dot{\gamma}_{||} \geq 10 s^{-1}$  approximately constant values of 0.7 and 1.2 Pa·s, respectively. In the case of isotropic solutions, the longitudinal and transverse viscosity components are about the same in this experiment.

Thus, we may presume that the presence of viscosity anisotropy for lyotropic polymer systems is experimentally proved. Let us now consider the typically polymeric dependences of the rheological characteristics in a steady-state shear flow: from shear stress, polymer concentration in solution, and temperature in terms of the peculiarities of the phase equilibrium in a polymer-solvent system. A substantial role is played by the viscosity anisotropy in these dependences. Let us analyze first the LC-solution flow curves.

### LC-solution viscosity vs. shear stress

As was stated above, no viscosity anomaly was practically observed in low-molecular isotropic single-phase systems. As for liquid crystals, it is another thing. In those systems, the effects of rheological nonlinearity are known in conditions of measurement of viscosity of specially non-oriented texture localized in low shear stress regions. The reason for such nonlinearity has long attracted the attention of researchers. As a result, there occurred the conception of viscoplastic behavior of liquid crystals, i.e., about the presence of a sufficiently strong structural network in LC, whose destruction, and the transfer of the system into a flow state, would require a definite amount of energy (yield stress). By way of example of low-molecular cholesteric LC-systems, a hypothesis emerged relating the flow curve shape to the texture transformations on shearing.

A more complicated situation develops with respect to the LC-polymer systems. The matter is that the isotropic polymer system is also nonlinear. However, in contrast to low-molecular liquid crystals, it is of the non-Newtonian type at high stresses. The scheme of the flow curve shape evolution with accumulation in the system of LC-phase and then the appearance of the crystal-solvate phase (similar to filled systems) can be seen in Figure 6. The experimental results for sulfuric acid solutions based on PPTA are given in Figures 7 and 8 (according to Reference 24).

The isotropic polymer solutions show typical flow curve shapes with zero shear and apparent (structural) viscosity sections. A dramatic change occurs in rheological properties with a 10% concentration of PPTA where there appears a LC-phase in the system. In this case, the absolute viscosity values decrease and the flow curve changes in shape: there appears a sharp decreasing branch  $\eta$  with increasing  $\tau$  different for different stress regions. This leads to the occurrence of a small shoulder at  $\log \tau \approx 2.6-3.0$  which expands with increasing concentrations so that the flow curves start to approach a Newtonian case. When the CS appears ( $C \approx 22\%$ ) again a rise in the viscosity is noticed in the region of the low  $\tau$ , and a slope of the flow curve on the whole. This is well seen in the three-dimensional diagram  $\log \eta$ - $\log \tau$  in Figure 8.

The data presented do not allow us to confirm the existence of a more appreciable viscosity anomaly of LC-solutions in comparison with the isotropic. A strong distinction from the linear behavior is recorded in the biphasic regions of the phase diagrams (I + LC) and (LC + CS). In this connection it is quite probable that the presence of a phase heterogeneity enhances the viscoplastic behavior effect. But is "viscoplastic" the best choice of word?

### On the mechanism of polymer liquid crystal flow

At the present time, the flow curve shape with three sections is generally recognized for LC polymers (Figure 9). This was described in our papers,<sup>12,25,26</sup> in Asada's publications with co-authors,<sup>27,28</sup> etc. On the basis of such a form of dependence  $\eta(\tau)$ , the flow mechanism for Section I is of a principal matter. According to data presented by different authors, this section is concerned with the presence of a viscoplastic behavior with a yield stress<sup>12,23,26</sup>; the influence of the mechanical and

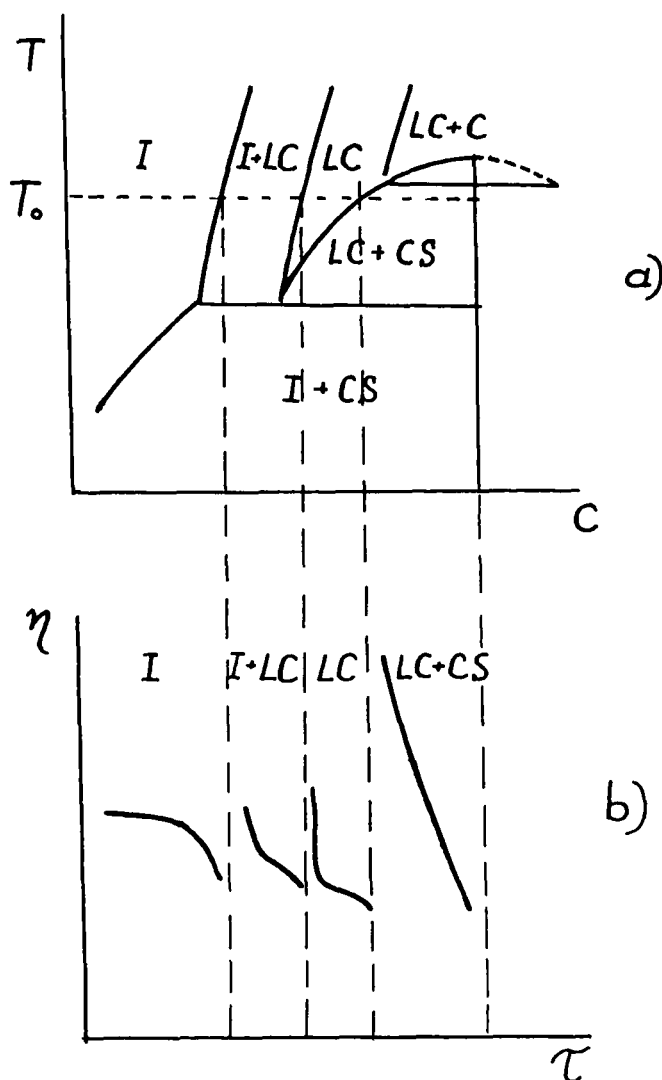


FIGURE 6 Schematic phase diagram of the system: aromatic polyamide-acid (a) and the flow curve shapes, corresponding to different diagram sections (b).

thermal pre-history<sup>29,30</sup>; domain (poly-domain) flow without varying<sup>12,27</sup> and with varying the dimensions and number of domains<sup>31</sup>; the influence of the initial texture of the sample.<sup>32</sup> The latter hypothesis seems especially interesting in the following interpretation.

Apparently, in nematics, the transmission of the processes of the movement momentum will be slowed down on the disclinations. This follows from the necessity of overcoming the LC-matrix strength which, strange as it seems, is greatest on these defects. A certain amount of energy is spent for this purpose which is expressed in a real value of yield stress. In other words, the disclinations will impose

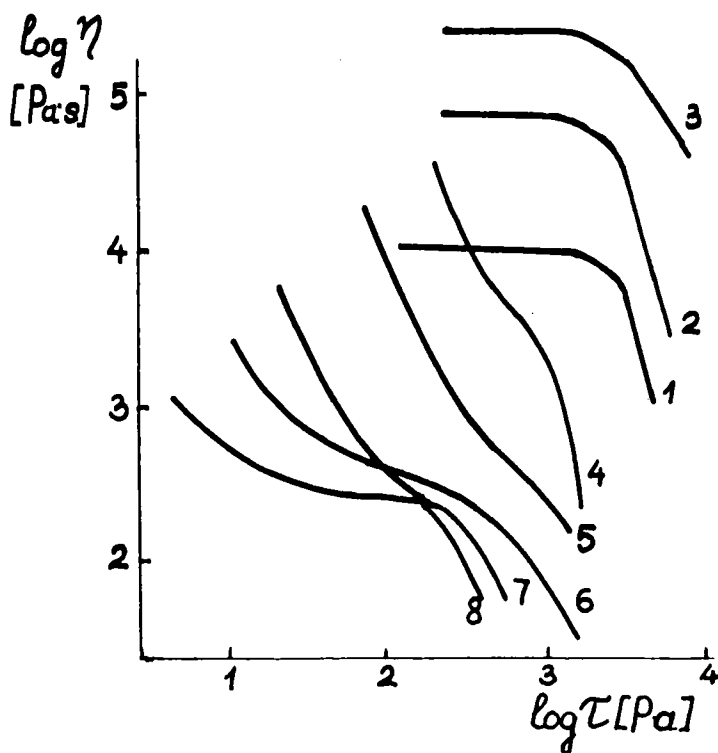


FIGURE 7 Flow curves of copolymer solutions based on PPTA concentration: 7(1), 9(2), 10(3), 11(4), 13(5), 19(6), 21(7) and 22% mass (8).

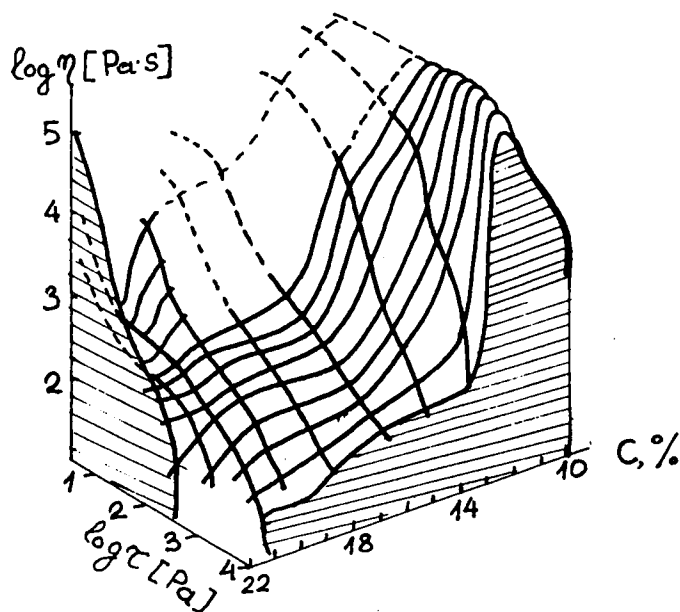


FIGURE 8 Diagram of  $\log \eta$ - $C$ - $\log \tau$  for sulfuric acid copolymer solutions based on PPTA at 80°C.

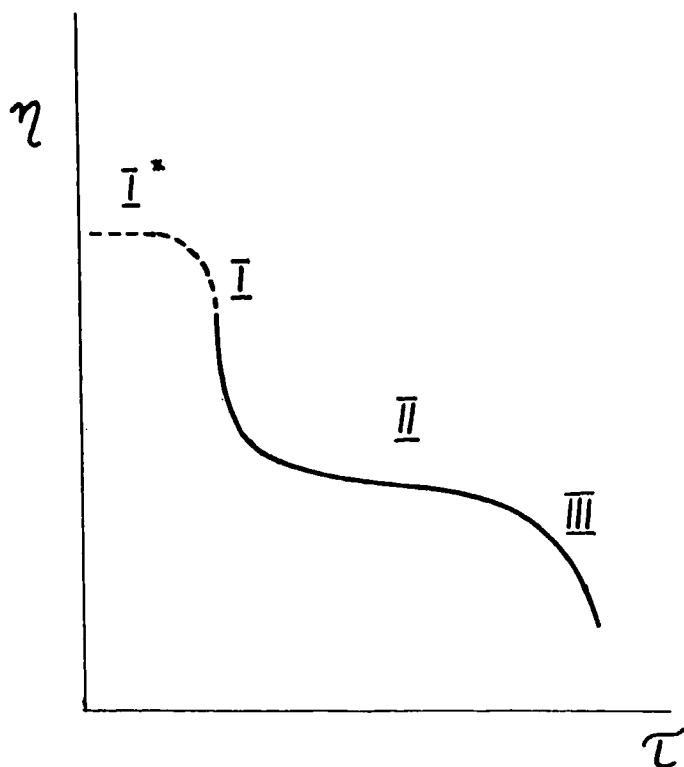


FIGURE 9 Schematic flow curve of the polymer liquid crystals (see explanation in the text).

a restriction on the propagation of the homogeneous area of the viscous flow with similar molecular orientation. Since the overwhelming majority of experiments with 100% LC-phase record a viscosity growth branch with decreasing stresses, but not the yield stress proper, we can imagine the conditions when the action times become so large (the deformation rates being small) that they will be compared with the disclination relaxation times. Under such conditions the system can flow with an undestroyed structure (creep regime) and the inhomogeneities will also move in a slow stream (see dotted lines in Figures 8 and 9). At higher rates, the disclinations already play the role of quasi-crosslinks structuring the solution. However, the molecular orientation increases gradually and the number of disclinations decreases, leading to a decrease in the viscosity. Concurrent with this, the viscosity anisotropy plays an important role in the transition region from Section I to Section II, which also favors the decrease in the total coefficient of the internal friction.

Hence, the contribution of the phase heterogeneity to the viscoplastic behavior (in the I + LC and LC + CS regions of the phase diagram) becomes more clear. The phase inhomogeneity of the system enhances the viscoplasticity effects due to the interphase phenomena which, in the framework of the suggested conception, are the restrictions of local mobility of a higher order than that of disclinations.

Thus, there develops a hypothesis concerning the determining role of the disclination system in the viscoplastic behavior of liquid crystals, which envisages the

presence of a Newtonian flow-branch (creep) at very low rates and shear stresses (Section I\*). Then, Section I will correspond to the orientational decline in the viscosity, whereas Section II will correspond factually to the monodomain (quasi-Newtonian) flow. LC fragmentation and nonlinear effects associated with it may appear in Section III.

The possibility of obtaining ideal oriented macrovolumes of LC-polymer systems should be taken into account. Such an orientation was not achieved in the case of a steady-state shear flow (as a rule, the mean angle of disorientation is as high as  $30^\circ$ <sup>20</sup>). The production of a liquid crystalline monodomain would seem possible in conditions of an additional superorientation of a thin layer of PBA LC-solution after cessation of a slow flow.<sup>19,33</sup> Such a process may be characterized by the anomalous increase of the dichroic ratio of one of the  $\pi$ -bonds of PBA during the relaxation process (Figure 10). However, the ultimately-oriented solution layer appears to be unstable and dissociates into a system of parallel strips (domains). The driving force of this process is still obscure, but it is quite possible that electromagnetic effects participate in it. It was for this purpose that the term "domain" was introduced.

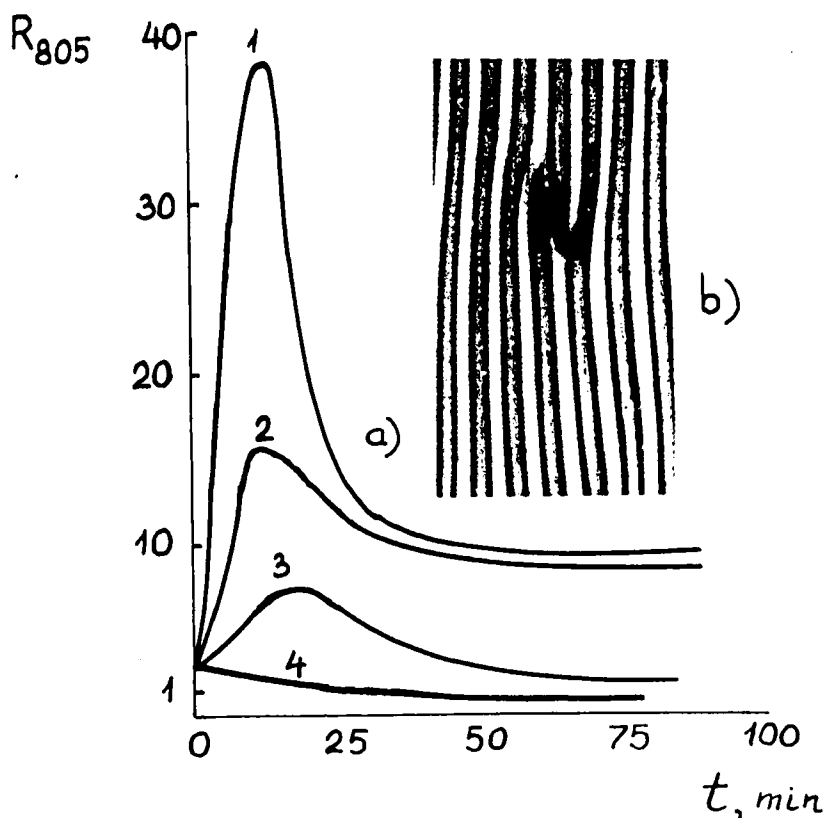


FIGURE 10 (a) A change in the dichroic ratio of the  $\pi$ -band  $805\text{ cm}^{-1}$  at relaxation after stopping the steady-state flow at  $\dot{\gamma} = 1.08(1), 1.68(2), 16.40(3), 96.00\text{ s}^{-1}(4)$ . (b) The schematic picture of the strips (domains).

As far as the rheological domains are concerned, we generally have in mind two kinds of microvolumes in LC. First, the microvolumes are limited by disclinations (i.e., the surface disclinations which are thermodynamically unstable in the absence of an outer field<sup>34</sup>). Second, by domain we have in mind the configuration of the director field involving a set of disclinations without their predominant orientation when averaged by volume.<sup>31</sup> This approach is a model for describing the rheological characteristics, for example, only the decrease in the size (an increase in number) of the domains without changing their internal structure is implied for Section I of the flow curve; this allows making the appropriate calculations.

A similar model of the initial flow stage can be employed also in the "disclination" hypothesis. However, it is necessary to take into further account the change in a number of disclinations as a result of the orientational process. Then, within the framework of the hypothesis concerning different flow curve sections, it is possible to systematize the principal cases for the flow of the LC-polymer systems and draw up certain, not too contradictory, hypotheses bringing us closer to understanding the mechanism of their flow. These hypotheses involve such concepts as a) the existence of disclination systems which should be destroyed in order to achieve a molecular flow; b) the macromolecular orientation in the shear field and decline in viscosity as a result of this process; c) the role of the interface boundaries in mixtures of LC-phase with isotropic and crystalline phases restricting the steady-state flow; d) the specific rheological nonlinearity of the LC-polymers due to viscosity anisotropy and relaxation time anisotropy, etc.

These peculiarities of rheological behavior should be borne in mind in processing LC-polymers.

### Dependence of viscosity of stiff-chain polymer solutions on concentration and temperature

On the basis of the hypothesis on the determining role of viscosity anisotropy in the viscoplastic properties of LC-polymers, we may observe in the  $C^*$  region a maximum in the dependence  $\eta(C)$ . However, the possibility of the existence and absolute value  $\eta_{\max}$  is determined depending on which section of the flow curve the viscosity has taken. Usually the comparison is made for Section II.

Figure 11 exhibits the dependence  $\eta(C)$  for copolymer solutions based on PPTA whose flow curves are given in Figure 7. For anisotropic solutions the dependences  $\log \eta$  ( $\log C$ ) were plotted at  $\log \tau = 2.0, 2.7$  and  $3.2$ , respectively. In the region of small  $C$ , the exponent  $\beta$  is practically equal to unit. At concentrations  $0.2$ – $0.7\%$  mass, a transition takes place from a power dependence with  $\beta = 1$  to the corresponding dependence with  $\beta = 4.2$ . Such a transition is usually associated with the formation of a fluctuation network of contacts. The value  $\beta$  in this region is lower than that in flexible-chain polymer solutions (5–6), this was indicated in Reference 35. At  $C > 6.5\%$ , a stronger power dependence of viscosity on concentration with an exponent  $\sim 6.0$  is observed. The literature offers close figures:  $6.8^{14}$  and  $5$ – $8$ ,<sup>36</sup> but for all the concentration regions between  $C_c$  and  $C^*$ .

Near  $C^*$ , the determining influence on the viscosity growth rate with increasing concentration is exerted by the heterophase fluctuations with a casual macromo-

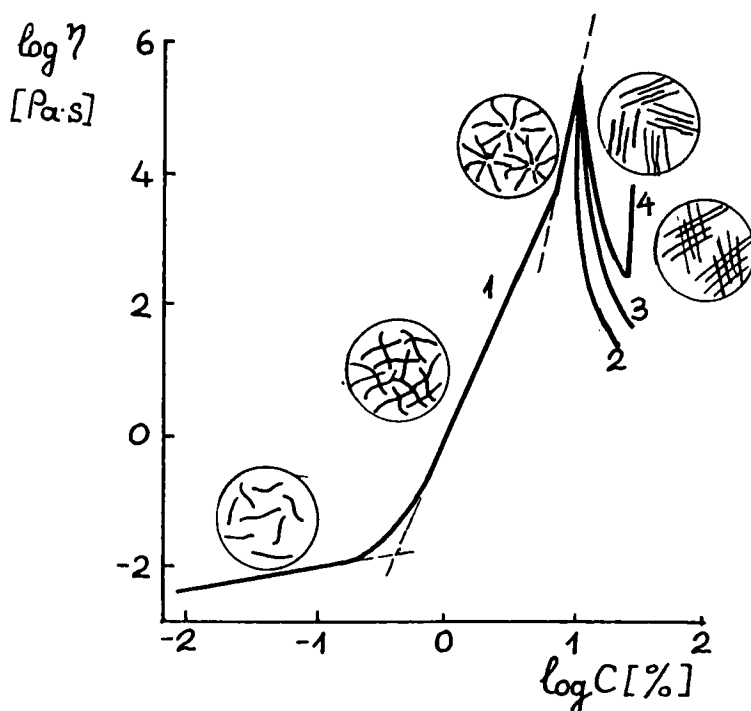


FIGURE 11 The concentration dependence of PPTA copolymer solution viscosity (1) in the Newtonian flow region and (2) at shear stresses of 100, (3) 5000 and (4) 30,000 Pa. Signs due to the morphology of the solutions are schematically shown in the circles.

lecular orientation<sup>24</sup> and the possible appearance of LC-phase traces at  $C$  by 0.5–1.0% lower than  $C^*$ <sup>26</sup> or at  $\frac{1}{2}C^* < C < C^*$ .<sup>35</sup> The pre-transient phenomena may lead either to an increase in  $\eta$ , as in this case, or to its decrease.<sup>37</sup> Possibly, the reason for such a behavior is due to the morphology of the fluctuation or phase formations at  $C \rightarrow C^*$  which may be spherulitic (as is seen in Figure 11) or fibrillar.

At  $C > C^*$ , there occurs a sharp viscosity decline, if it is measured on Section II. First of all, this is due to the orientation effects (viscosity anisotropy). However, if we plot a dependence  $\eta(C)$  in comparison with the phase diagram of the system and take viscosities measured on Sections I, II and III, we will visualize a more complicated picture (Figure 12). At stress  $\tau_I$  the viscosity with the appearance of a LC-phase enhances drastically, while with the disappearance of the texture defects, the curvature of the branch  $\eta(C)$  should decline gradually and couple with the dependence  $\eta(C)$  for  $\tau_{II}$  in the long run. In such conditions the dependence  $\eta(C)$  bears an ordinary character for LC-systems with maximum at  $C^*$ . At stress  $\tau_{III}$  the dependence  $\eta(C)$  does not reveal a maximum at  $C^*$ , but rises monotonically with increasing concentration. In all likelihood, at high  $\tau$ , the difference between the isotropic and anisotropic phases disappears due to fragmentation down to molecular sizes of the anisotropic phase. For this reason, the curve 3 is a limited case of quasi-Newtonian viscosity at  $C > C^*$  (for 100% of the LC-phase) if, of



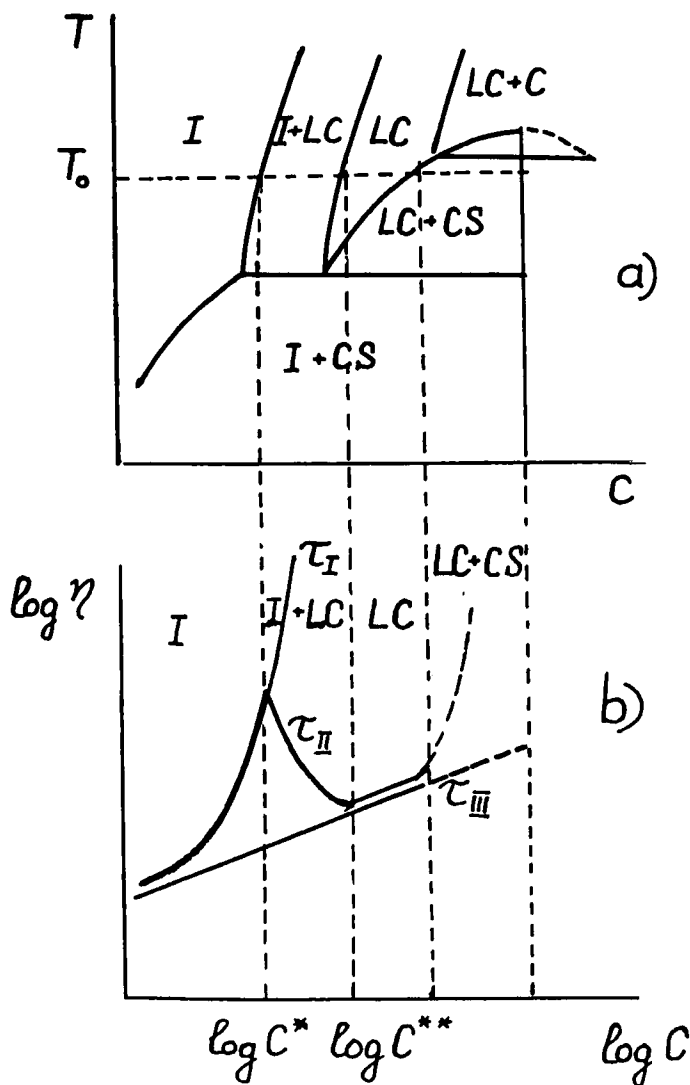


FIGURE 12 (a) Schematic phase diagram and (b) concentrational viscosity dependence corresponding to different sections of the flow curves. (See explanation in the text).

course, at high  $C$  no new phase transition takes place, for example, the appearance of crystal-solvates.

The external nature of the dependence  $\eta(C)$  at  $\tau_{II}$  is the best visual evidence of the peculiarities of the rheological properties of the LC-polymer systems. The presence of the viscosity maximum often serves as a criterion for attributing the system to a liquid-crystalline one, under conditions when other characteristics, in particular birefringence, cannot be interpreted unambiguously.<sup>38</sup>

Practically, the same situation is known also for the temperature dependence of viscosity which is of a similar type of lyotropic as well as for thermotropic systems. At the transition point from LC to an isotropic state, the viscosity has a maximal value, due to the transition from an ordered to an unordered system. The presence of a maximum for low-molecular LC is usually revealed during liquid crystal flow with an uncontrollable orientation. If we single out the coefficients corresponding to the macromolecule orientation parallel to the velocity and parallel to the shear rate vector ( $\eta_{\parallel}$ ), one can arrive at certain generalizations. The maximum in the nematic–isotropic phase transition region for *p*-azoxyanisol is observed for dependences  $\eta(T)$  and  $\eta_{\parallel}(T)$  (Figure 13a). A bend is observed on the dependence  $\eta_{\perp}(T)$  in the transition region.<sup>39</sup>

In the case of nematic polymer solution, the viscosity (at  $\tau_{II}$ ) changes upon transition from point  $\chi$  as  $T$  decreases through different regions of the phase diagram, as is seen in Figure 13b. The dependence presented looks like the one given for *p*-azoxyanisol with the exception of two things. First, for low-molecular thermotropic liquid crystals there is no mixture region of the isotropic and anisotropic phases, the presence of which leads to a smoother decline in the viscosity of the polymer systems as the LC-phase begins to accumulate. Second, the occurrence of the CS leads to a sharper increase in the viscosity with decreasing temperature than when it is prescribed by the flow activation energy in the 100% LC-phase region (the occurrence of a crystal solvate is not a regular case).

In order to have an idea of the activation characteristics of the flow process of the LC- and isotropic phases, let us consider the activation energy dependence on concentration for a copolymer solution based on PPTA (Figure 14). Typical of this dependence are the increase in the curvature in the pre-transient region and a sharp decline in  $E$  at  $C > C^*$ . With a transition to a LC-state,  $E$  declines three-fold in the concentration range of 1%. For LC-solutions, the temperature coefficients for viscosity are in general the same for different concentrations. This fact can indicate that the same kinetic flow unit (domain) in the region of the quasi-Newtonian flow is preserved, which is typical of the uninterrupted LC-phase systems.

### Macroscopic elasticity of LC-polymer systems

Besides viscosity, high-elasticity plays an essential role in LC-solution processing. But before discussing the behavior of the lyotropic systems in the process of spinning, let us consider the high-elasticity characteristics of polymers produced in model experiments. This is usually the first difference of normal stresses ( $N_1$ ) and elastic deformation ( $\gamma_e$ ).

The appearance of LC-phase in stiff-chain polymer solutions causes a drastic change in their elastic properties. Thus, if in ordinary (isotropic) flexible- and semi-stiff-chain polymer solutions, the value  $N_1$  is proportional to  $\dot{\gamma}^2$ , then it is often proportional to  $\dot{\gamma}$  for LC-systems. Moreover, for anisotropic polymers, there is a shear rate interval inside of which  $N_1$  assumes negative values.<sup>29,40</sup> In a

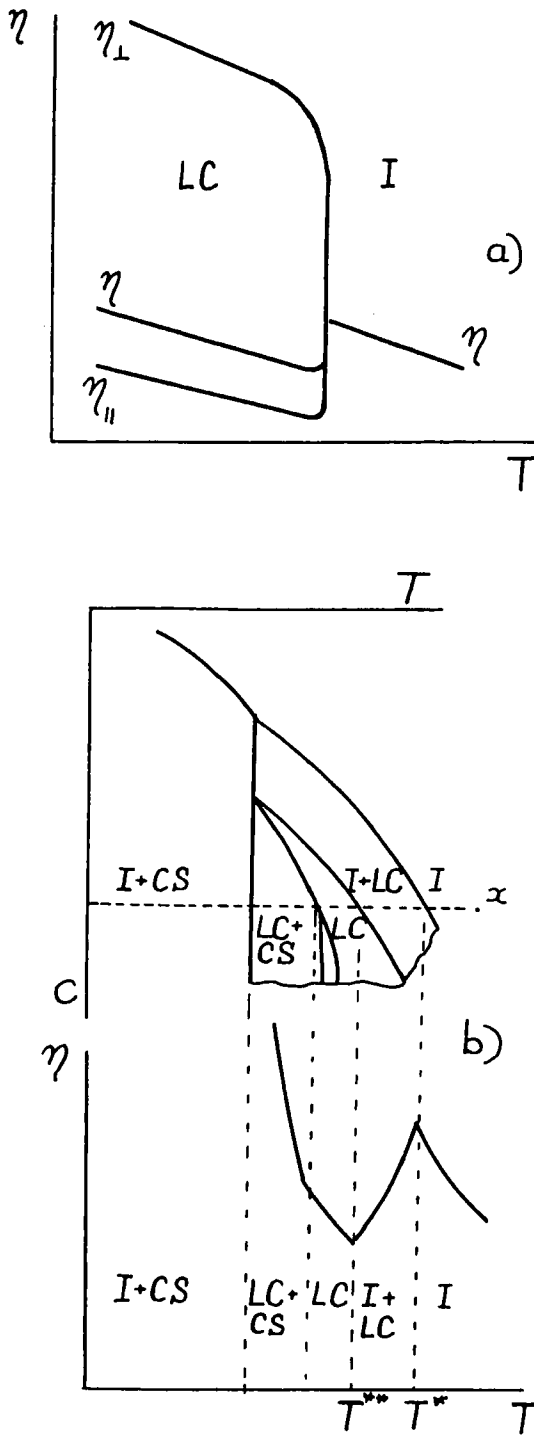


FIGURE 13 The temperature dependences of the anisotropic viscosity coefficients (a) *p*-azoxyanisol as well as (b) stiff-chain polymer solutions in different phase diagram regions.

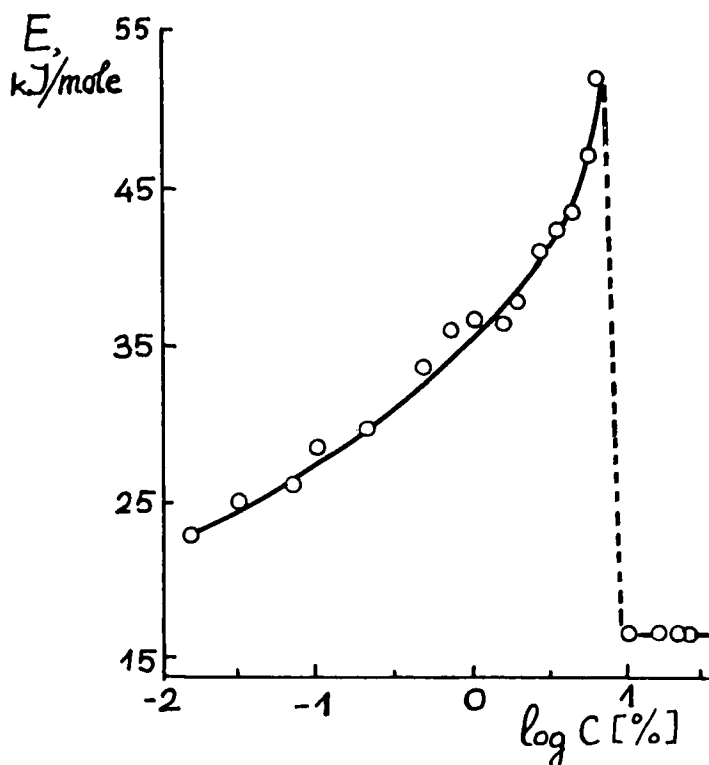


FIGURE 14 The dependence of the flow activation energy of the PPTA solutions in  $\text{H}_2\text{SO}_4$  on concentration.

number of cases,<sup>29,41</sup> the negative values  $N_1$  were obtained also in the transition regimes of deformation and were associated with the mechanical pre-history of the sample.

In our opinion a no less important role is played by the textural inhomogeneity or molecular orientation in analyzing the measurement results of the normal stresses. Indeed, besides viscosity, the existence of anisotropy of other rheological characteristics which are also tensor values should be borne in mind. Therefore, uncontrollable orientation, uncertain boundary conditions on the measuring surfaces both in deformation and in relaxation generate ambiguity in defining the absolute normal stresses values.

Nevertheless, low and even negative values  $N_1$  exist, because small values for the swelling of the LC-polymer extrudates<sup>29</sup> or even their contraction<sup>42</sup> have been recorded for LC-polymers. This fact is associated with the existence of the yield stress and helps in securing and even perfecting the molecular orientation in a free jet as compared to the one developed in the channel flow. Thus, in the case of spinning of LC-solutions and melts, we may expect a dependence of the molecular orientation in the fiber, and consequently, its strength, depending on the conditions of their flow in the spinneret orifices.

## PECULIARITIES OF SPINNING FROM LC-POLYMER SOLUTIONS

Wet-spinning is a complicated, multifactor process involving simultaneously the rheological, phase and structural changes as a result of heat-mass transfer of the spin dope jet with a liquid coagulating bath. However, before going into a more comprehensive analysis of the behavior of the spinning fiber in a coagulating bath, let us consider one more stage inevitably associated with any process of shaped articles production, viz., the flow through narrow channels. Some of the problems of jet-formation for LC-solutions were discussed above where the low expansion factors for their extrudates were emphasized. In this part of the review it is reasonable to draw the reader's attention to two aspects of the problem: orientation effects and efflux stability.

First, let us consider the kinematic peculiarities of the polymer flow from the reservoir into the channel (Figure 15). The primary converging flow occurs in zone I where the shear and extension deformations coexist (part of the extension increases while moving to the stream axis). Irregular vertical currents are present in zone II (secondary flows) and it is desirable to separate them from the main flow by rigid walls by employing a conical entrance part. Uniaxial extension is a much more orienting kind of deformation than the shear. In the previous part of this paper the main attention was focused on the shear flow. It is in this regime that LC-polymers are usually investigated, although, undoubtedly, new rheological and structural effects can be observed in the longitudinal flow. Thus, a "negative longitudinal viscosity" was detected in the thermotropic cellulose system.<sup>45</sup> In similar hydroxypropylcellulose as well as in mesophase poly-*bis*-trifluorethoxyphosphasene polymers the extensional deformation at the channel entrance gives rise to fibrilization of uniaxially oriented extrudates (a kind of self-reinforcement).<sup>42-44</sup>

For a long time the literature discussed the problem of optimal geometrical characteristics of the spinneret channel,<sup>45</sup> generally dealing with the size of the inlet cone angle  $\alpha$  and ratio of the length of the cylindrical part  $L$  to the diameter  $D$ . From the viewpoint of maintaining the developed orientation at the expense of extension of the system at the entrance to the channel in the free jet, long channels do not seem to be suitable. We may arrive at such a conclusion by analyzing the distribution of the stresses in a flow using the rheo-optical techniques. This method renders it possible to record lines of equal differences in the main stresses (isochromes) in polarized light. For the flow axis, these lines can be recalculated into tensile stresses  $\sigma_{11}$ :<sup>47</sup>  $\sigma_{11} = n\lambda/Cw$ , where  $n$  is the ordinal number of isochromes,  $\lambda$ , the wavelength of the monochromatic radiation;  $w$ , the solution layer thickness in the slit channel supplied with transparent walls; the  $C$ -dynamo-optical coefficient is assumed constant. As the optical anisotropy of the segments increases, which, as a rule, accompanies a rise in stiffness, the value  $C$  grows.

Let us compare<sup>46,47</sup> the isochrome pictures of the three channels with different entrance parts, different lengths but with the same diameters (Figure 16). The isotropic solution flow of semi-rigid-chain polyamidebenzimidazol (principally giving also LC-solutions) through a  $180^\circ$  channel inlet angle is accompanied by the occurrence of stress concentrations on the edges. No such concentrations were

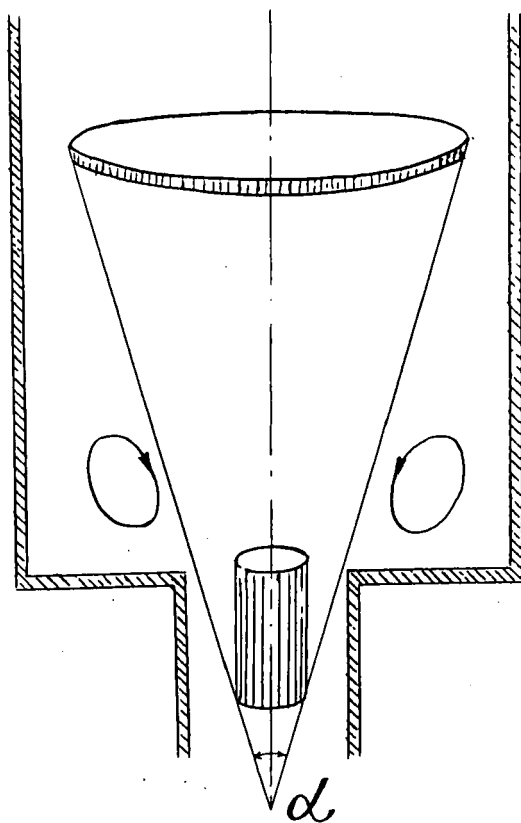


FIGURE 15 The scheme for explaining the existence of extensional deformation in the channel entrance.

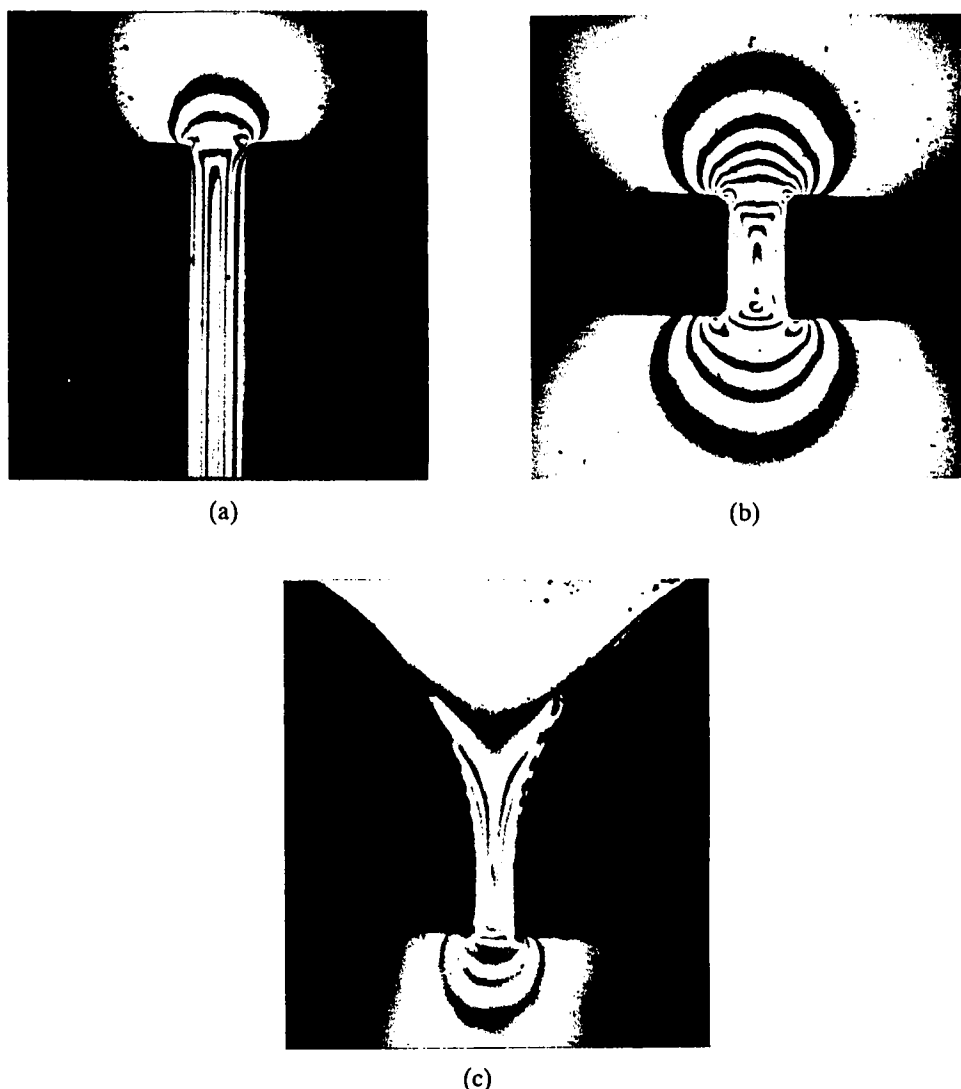


FIGURE 16 Isochrome picture of polyamidebenzimidazole solutions during the flow through channels of diverse shapes a)  $\alpha = 180^\circ$ ,  $L/D = 28.6$ ; (b)  $\alpha = 180^\circ$ ,  $L/D = 1.5$ , c) channel with a radius rounding in the inlet part,  $L/D = 1.5$ .

observed for smooth inlet channels (or a gradually varying cone angle), which contributed to the realization of the undistorted extension field.

The calculated profiles  $\sigma_{11}$  along the stream axis  $Z$  (positive  $Z$  is referred to the entrance part, the negative to the plane-parallel part of the split) are given in Figure 17. Taking into account the accepted allowance for the dynamo-optical coefficient constancy, the same regularity will be apparently observed for LC-solutions. For them, however, it is extremely complicated to separate the induced anisotropy (photoelastic effects) from the anisotropy inherent in liquid crystals. The values

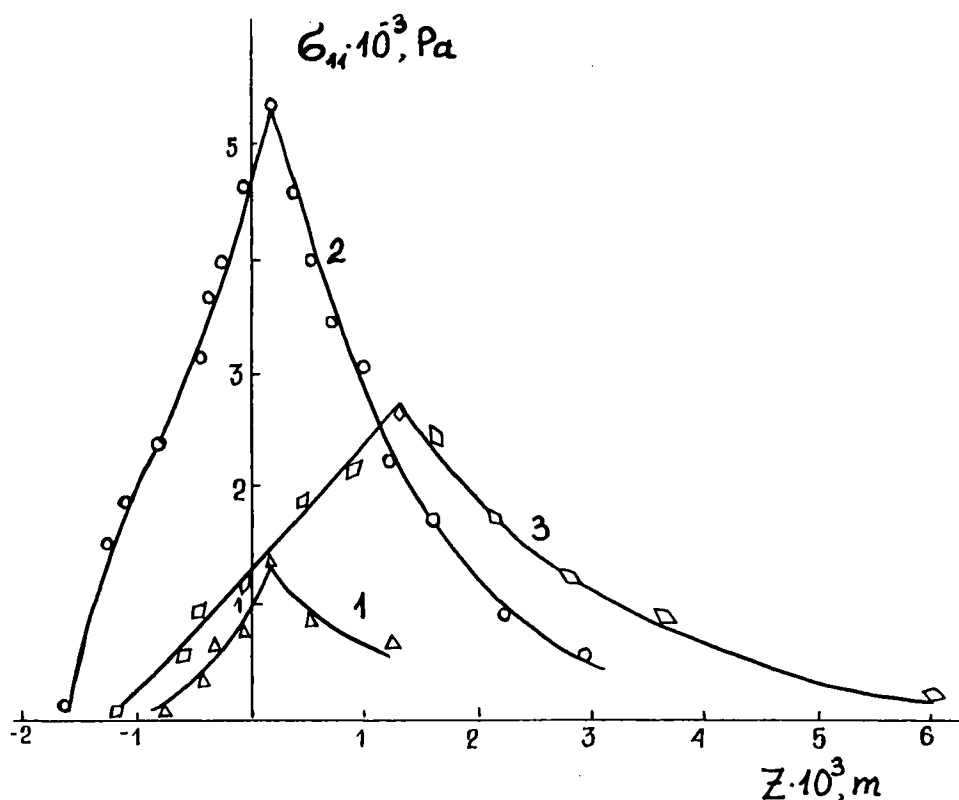


FIGURE 17 Profiles of the tensile stresses along the channel axis for (a) 1, (b) 2, (c) 3 channels of Figure 16.

$\sigma_{11}$  for the long canals are significantly lower, but their relaxation occurs earlier (at a distance of  $\sim 1$  mm below the edge). As to short channels, it is possible to maintain the tensile stresses prior to the outflow of the jet from the channel. In this respect, channels of varying taper angles (which should not exceed the inlet angle  $\alpha$  in the middle part) appear to be more favorable for the increment and relaxation in this case proceed smoother than in the flat inlet part.

A sharp increase in  $\sigma_{11}$  as in the case of channel b can hardly bear sense because of the possible exceeding of the cohesive strength of the solution or the occurrence of an unstable flow.

As to instability, we shall now direct our attention to the second part of the problem: the stability of the jet formation. In order to promote a stable jet formation, it is necessary to have long channels. However, in this case, because of the existence of diagonal components of the stress tensor there can be a serious loss in the molecular orientation. Even if the values exceed the solution strength at the inlet part, this defect in long channels can be remedied by relaxing the extensional stresses, whereas, in short channels, it can cause a disturbance in the regularity of the jet at moderate rates. This is outwardly expressed in its helicity.<sup>48</sup> Therefore, it is necessary to find a sensible compromise between orientation and



stability, which in each special case conditions the choice of definite channel geometry. Recall that the expansion factor of the LC-solution jet is very small and it changes little with the channel length. Therefore, the achievement of a high orientation in the flow for these systems can be directly associated with the orientation in the as-spun yarn. Then the role of the coagulating liquid is to ensure a rapid fixation developed in the liquid state of the structure.

The jets of the dopes pass into the coagulating liquid either directly (the spinneret is submerged in the bath) or through an air gap. When regarded from general positions, such a layer is necessary for the separation of a hot spinning solution with  $T > T_m$  CS from a cold bath. However, it influences also the spinning kinematic. If it is impossible to achieve high-draw ratios in wet-spinning ( $\Phi = V_2/V_1$ , where  $V_2$  is the wind-up rate, and  $V_1$  is the throughput rate from the channel), then the values  $\Phi$  in the dry-jet wet process can be substantially higher at the expense of the longitudinal deformation of the liquid jet in the air gap. This renders it possible to enhance the wind-up and produce thinner yarns, but it is hardly possible that it will bring about a rise in tenacity. If it is able to produce a well oriented jet from spinneret orifices, then it is sufficient to provide a small draw ratio in the coagulating bath ( $\Phi = 1.7-2.0$ ) for achieving an ultimately strong (without taking into account subsequent thermal treatment and thermal drawing) fiber.<sup>49</sup> It is important to note that this is achieved at such an initial solution concentration that it becomes totally liquid-crystalline (Figure 18).

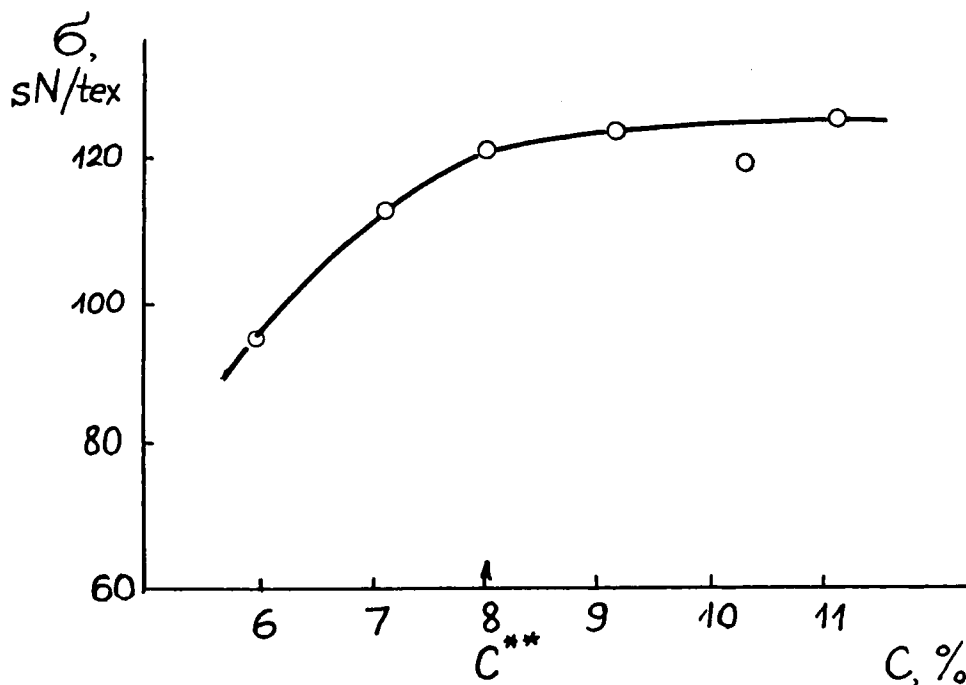


FIGURE 18 The dependence of the relative strength of the as-spun PBA-fibers on the concentration of the spinning dopes.

The rise in the wind-up rate in the air gap variant is restricted by the so-called "draw resonance." The resonance phenomenon consists of a periodic variation of the jet diameter starting from the critical draw ratio,  $\Phi_c$ . This phenomenon was repeatedly observed in melt spinning,<sup>50</sup> and in recent years in dry-jet wet spinning from isotropic solutions of polyoxadiazols and from anisotropic solutions of PPTA.<sup>51</sup> The outward appearance of the resonance is seen in Figure 19 illustrating successive flow stages of the jet in an air gap.

There exist diverse theoretical speculations concerning the description of the resonance phenomenon. We shall not consider these problems in detail, but shall present these positions from the point of view of the so-called "wave kinematics"<sup>52</sup> and the behavior of the system as an "unstable-state cycle."<sup>53</sup> In the first case, the resonance is regarded as the propagation of waves of the volume throughput along the spin-line. Second, it is regarded as a result of a metastable state of the jet under conditions of tensile stress action (a casual perturbation causes oscillational generation). As for the Newtonian systems, the value  $\Phi_c$  is predicted and supported experimentally as being equal to  $\sim 20$ ,<sup>50,52</sup> whereby the elasticity can have a destabilizing effect on the resonance occurrence conditions.

It would be useful within the context of this paper to indicate the means for controlling the resonance, but unfortunately there are no reliable methods at the present time. In the case of aromatic polyamide solutions, the resonance is partially inhibited by decreasing the air gap thickness, by the presence of a developed conical part at the channel inlet and a short cylindrical part, and by cooling the jet.<sup>51</sup> The connection between the behavior of the free jet and channel geometry gives evidence of an interrelationship between the stressed states in the deformed solution bulk and in the practically unidimensional jet.

The next stage of the process is concerned with the spinning fibers in the coagulating liquid. Neglecting the heat transfer processes (we can accept the conditions as being isothermal), let us concentrate our main attention on the non-solvent diffusion inside and the solvent diffusion outside the thread. These processes result in the evolution of the phase and relaxational states of the polymer system. If we assume that the phase and relaxation transitions are of a threshold character (with respect to coagulant concentration at a definite section of the thread), we may expect the existence of one or several fronts in the spinning fiber.<sup>54</sup> In a general case, the front separates the solution and a gel-like system is formed as a result of an incomplete decomposition spinning dope into phases. In concrete cases, high-elastic and glass-transition fronts are added to this front as well as a transition boundary to the system with complete phase separation (Figure 20).

If the gelation front in a wet-spinning process is practically closely adjacent to the spinneret, the regime is "rigid," but if there is a liquid interlayer between the front and the spinneret, the spinning is "soft."<sup>46,54</sup> The existence of the dramatic changes that occur in the relaxation states were proved by the results derived from the comparison of the rate of travel of the optical boundary on the model dope drop, surrounded by the coagulating liquid, with the existence of typical dependences of the thread friction coefficient, deformation capability, tenacity of as-spun fibers, etc., on the distance from the spinneret.<sup>55</sup> The recalculation of the time

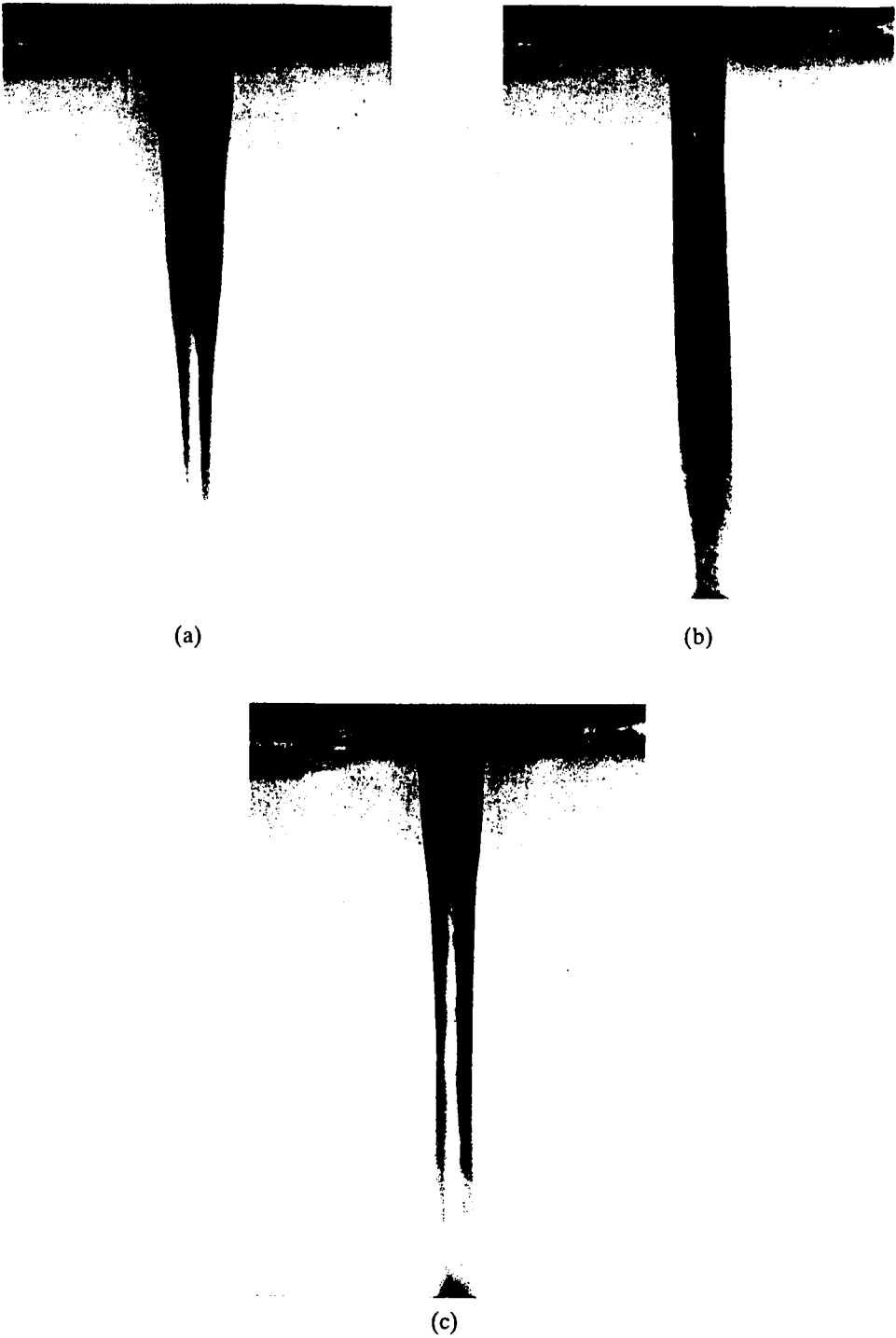


FIGURE 19 Subsequent stages of photographs of the jet shape of PPTA-solution in the air gap.

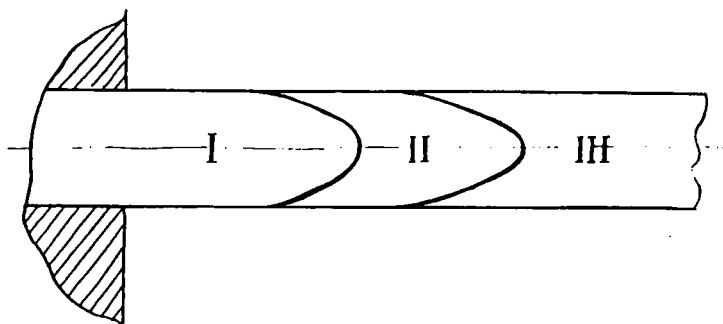


FIGURE 20 Hypothetic scheme of distribution of physical states in the spinning thread: I, solution; II, gel-like state; III, state with completed decomposition into the phases.

necessary for the boundary to reach the drop center over a distance along the spin-line is not a difficult task.

An arrangement fixed to a special spinning device is used for local deformation probing of the spinning thread (Figure 21). This apparatus is designed for measuring the force acting on the spinneret, ( $T_1$ ), and close to wind-up bobbin, ( $T_2$ ). The local probing is accomplished with the aid of a friction body which is made up of a fixed cylinder (6) and two moving rollers (5 and 5'). The rotation speed of the rollers renders it possible to determine the run-on ( $v_1$ ) and run-off speeds of the thread from the friction body ( $v_2$ ). Such an arrangement can be used not only for determining the friction coefficient and local deformaticity, it can also measure the current efficient modulus:

$$G = (T_2 - T_1) / S \ln v_2 / v_1$$

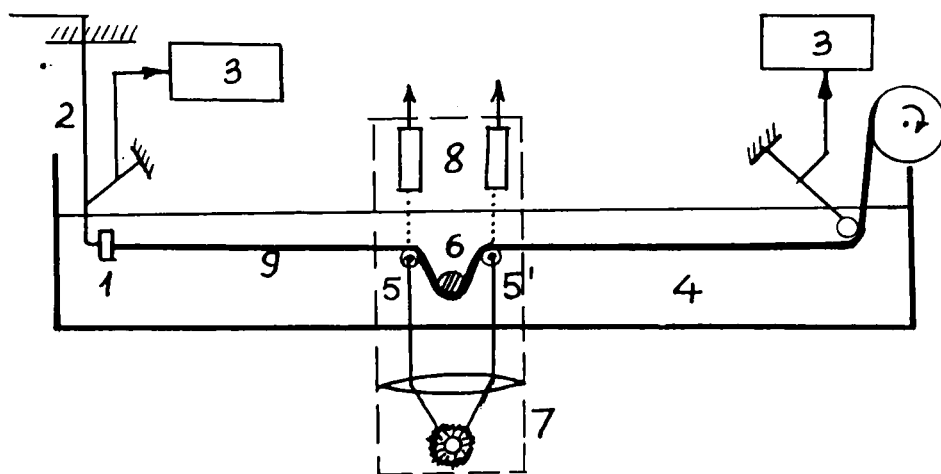


FIGURE 21 The scheme of the equipment for investigation of the wet-spinning process. 1, Spinneret; 2, transfer line for the spin dope; 3, force measurement system; 4, coagulating bath; 5 and 5', rotating rollers for measuring  $V_1$  and  $V_2$ ; 6, "friction body"; 7, light source; 8, photomultiplier; 9, spinning thread.

where  $s$ , is the thread cross-section area. As an example, the profile of the friction coefficients for the spinning yarns are shown in Figure 22. Their non-monotonic change can be seen.

The evolution of the phase states (LC and crystalline) is also possible within the framework of the relaxation states. This is more so, as shown, in local effect conditions. If the spinning solution were liquid-crystalline, the non-solvent concentration thresholds for its gelatinization would be very low.<sup>56</sup> This implies that the forming regime is "rigid" and the linear rate of the spinning thread immediately at the spinneret becomes equal to the wind-up speed. The drawing is concentrated at the very narrow section of the spinneret. Realization of the "rigid" spinning regime under conditions of high molecular orientation at the channel is a favorable factor, for it provides a fast fixing of orientation in the fiber.

On the other hand, if the molecules are not stiff enough for LC-phase formation in solution, such a transition can occur in the gel-like state, when the polymer content in the concentrated polymer phase exceeds  $C^*$ .<sup>26</sup> Then in the case of a prolonged transition kinetic and under deformation conditions there may appear an oriented LC-phase in the spinning thread. It is quite possible that, e.g., such a transition is related to the so-called "rheological jump" phenomenon which consists of a sharp increase of a force, acting on the spinneret ( $T_1$ ) at a definite draw ratio under wet spinning conditions.<sup>57</sup> The dependence of  $T_1$  on  $\Phi$  for polyamidebenzimidazol solutions in dimethylacetamide (DMAA) during spinning in a DMAA-water mixture ("soft" conditions) is given in Figure 23. It is quite probable that the transition of the system to a LC-state gives rise to a change in the whole series of its characteristics. Thus, the conditions for the polymer coagulation from the solution apparently vary because the cross-section of such fibers assumes a star-like shape.<sup>46</sup> The physicommechanical properties of the fibers also change substantially.

The part of this paper concerning the processing of lyotropic LC polymers has,

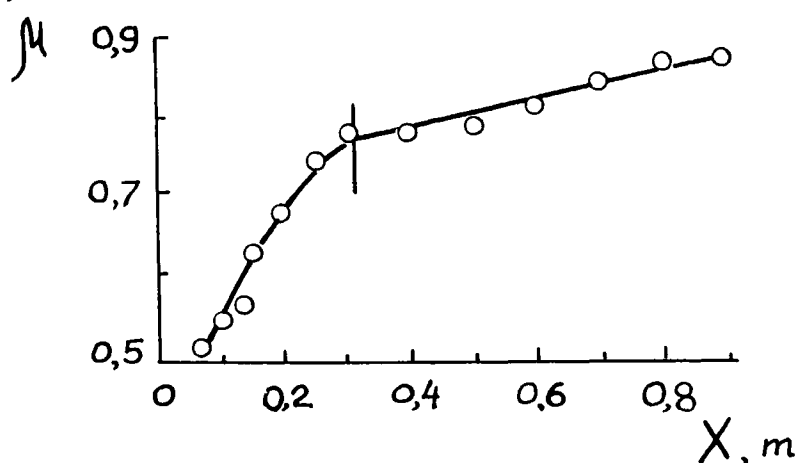


FIGURE 22 The dependence of friction coefficients on the friction body along the spinline. The solid line corresponds to the achievement of the coagulation boundary of the model drop center.

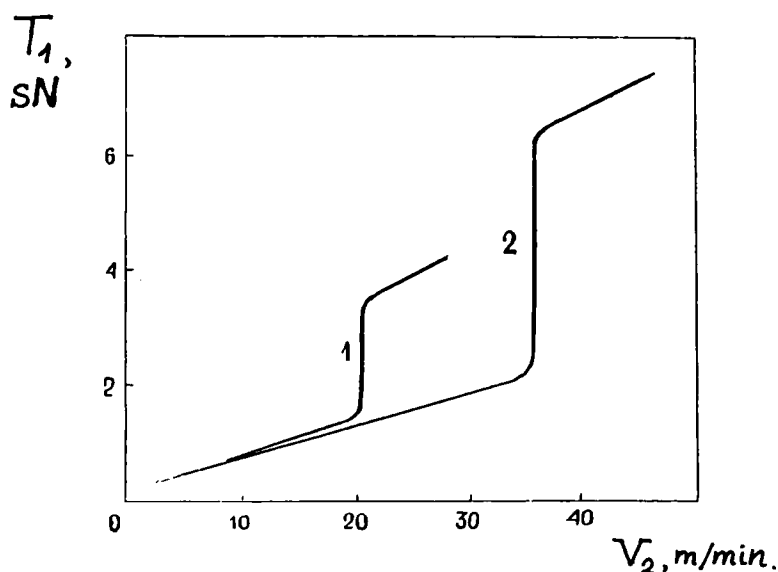


FIGURE 23 The dependence of a force acting on the spinneret on the wind-up rate for the throughput rate (1) 2.3 and (2) 6.8 m/min.

for certain reasons, been written in a schematic fashion. Following this principle further, we present the scheme for varying the parameter of the order

$$S = (3 \overline{\cos^2 \Theta} - 1)/2$$

( $\Theta$  is the mean disorientation angle of the long molecule axes relative to the fiber axis) along the spinline for LC and isotropic solutions (Figure 24). It is seen in the Figure that the high orientation for the LC-system (curve 1) already is achieved at the moment the solution flows out of the spinneret channel. Furthermore, it is sufficient to have a small difference in the wind-up and throughput rates to produce an ultimately oriented fiber (the heat treatment affects mainly the increase in the elasticity modulus).

For isotropic solutions of flexible-chain and semi-stiff-chain polymers the orientation is lower at all stages. The orientation factor can become less on the expansion region (in the free jet) than at the converging flow section (in the entrance to channel). The main increase in the orientation was observed in the coagulating bath (provided the transition is possible in a LC-state) and at the plastification (orientational) draw-down stage (positions II and III). In a number of cases, the transition to a LC-state occurs during heat treatment of as-spun fibers<sup>58</sup> (stage III). This case corresponds to the dotted dependence Section S(x).

For LC-solutions the completed orientation is achieved in the flow, i.e., in a state of free movement of the molecules or their segments. But in the spinning of fibers from isotropic solutions of flexible-chain polymers, the solidlike system undergoes drawing, which may lead to the occurrence of defects. In such a case we observe another advantage of using LC-spinning systems.

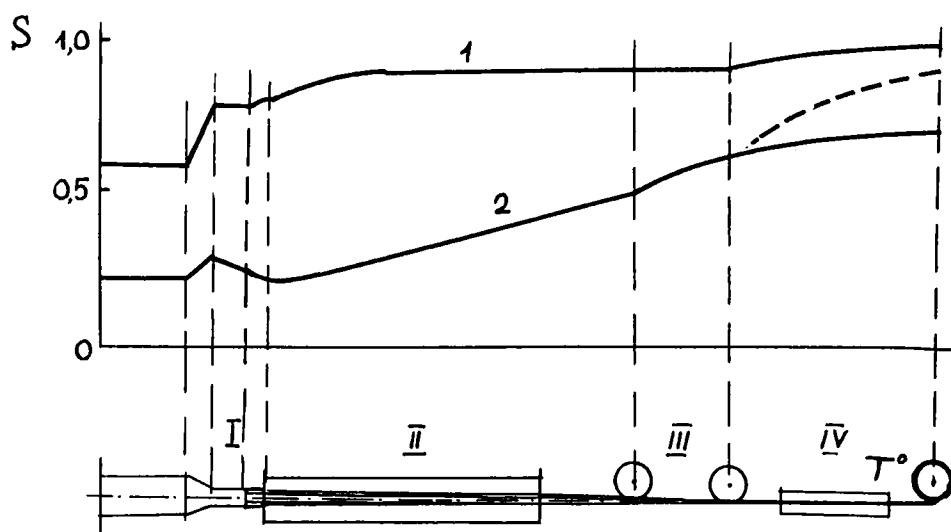


FIGURE 24 The scheme for changing the factor of orientation along spinline for (1) LC- and (2) isotropic solutions (see explanation in the text).

In drawing up a conclusion we may claim that lyotropic LC-polymers play an extremely important role in contemporary science and technology. The specificity of phase equilibria in lyotropic systems stimulated a great variety of theoretical and experimental investigations in this area. The singularity of the hydrodynamic properties has opened up new horizons for the investigation of theoretical and experimental rheology of anisotropic media. Finally, thanks to the remarkable orientation in the flow and the absence of the disorientation phenomena at the subsequent stages of spinning from LC-solutions, it is possible to produce small-defective super-high tenacity fibers. The strength of such fibers is as high as 500–550 kg/mm<sup>2</sup>, with the elasticity moduli as high as 20,000 kg/mm<sup>2</sup>.

## References

1. L. Onsager, *Ann. N.Y. Acad. Sci.*, **51**, 627 (1949).
2. P. J. Flory, *Proc. Roy. Soc.*, **234A**, 73 (1956).
3. W. G. Miller, C. C. Wu, E. L. Wee, G. L. Santee, J. H. Rai and K. G. Goebel, *Pure Appl. Chem.*, **38**, 37 (1974).
4. A. R. Khokhlov and A. N. Semenov, *Macromolecules*, **17**, 2678 (1984).
5. A. R. Khokhlov and A. N. Semenov, *Physica*, **112A**, 605 (1982).
6. "Liquid-Crystalline Polymers" N. A. Plate, ed., (Khimiya, P. H., Moscow, 1988, in Russian).
7. T. M. Birshtein and B. I. Kolegov, *Vysokomolekul. Soedin.*, **25A**, 2519 (1983).
8. V. G. Kulichikhin, V. A. Platonov, E. G. Kogan, A. V. Volokhina and S. P. Papkov, *Vysokomolekul. Soedin.*, **20A**, 2224 (1978).
9. S. P. Papkov, *Vysokomolekul. Soedin.*, **21B**, 787 (1979).
10. T. A. Kulichikhina, V. A. Platonov, N. V. Vasil'eva, E. G. Kogan, V. G. Kulichikhin, V. D. Kalmykova, A. V. Volokhina and S. P. Papkov, *Vysokomolekul. Soedin.*, **24A**, 964 (1982).
11. V. G. Kulichikhin, E. G. Kogan, A. Ya. Malkin and A. V. Volokhina, *Khim. Volokna*, **N 6**, 26 (1978).
12. V. G. Kulichikhin, "Orientation Phenomena in Polymer Solutions and Melts," A. Ya. Malkin and S. P. Papkov, eds. (Khimiya P. H., Moscow, 1980), Chap. 3, pp. 144–228 (in Russian).

13. S. P. Papkov, V. G. Kulichikhin, V. D. Kalmykova and A. Ya. Malkin, *J. Polym. Sci., Polym. Phys. Ed.*, **12**, 1753 (1974).
14. D. G. Baird and J. K. Smith, *J. Polym. Sci., Polym. Phys. Ed.*, **16**, 61 (1978).
15. V. N. Tsvetkov, "Newer Methods of Polymer Characterization," B. Ke, ed. (Interscience Publ., 1964), Ch. 14.
16. J. I. Ericksen, *Trans. Soc. Rheol.*, **11**, 5 (1967).
17. F. M. Leslie, *Proc. Roy. Soc.*, **307A**, 359 (1968).
18. Y. Onogi, J. L. White and J. F. Fellers, *J. Polym. Sci., Polym. Phys. Ed.*, **18**, 663 (1980).
19. V. G. Kulichikhin, V. A. Platonov, L. P. Braverman, A. V. Volokhina, A. Ya. Malkin and S. P. Papkov, *Vysokomolekul. Soedin.*, **18A**, 2656 (1976).
20. M. Miesowich, *Nature*, **158**, 27 (1946).
21. V. G. Kulichikhin, G. I. Kudryavtsev and S. P. Papkov, *Intern. J. Polym. Mater.*, **9**, 239 (1982).
22. V. S. Volkov and G. V. Vinogradov, *Vysokomolekul. Soedin.*, **26A**, 1981 (1984).
23. D. Marsh, J. Pochan, et al., *J. Chem. Phys.*, **58**, 5795 (1973).
24. V. G. Kulichikhin, V. A. Platonov, L. P. Braverman, T. A. Rozhdestvenskaya, E. G. Kogan, N. V. Vasil'eva and A. V. Volokhina, *Vysokomolekul. Soedin.*, **29A**, N 12 (1987).
25. S. P. Papkov, V. G. Kulichikhin, A. Ya. Malkin, V. D. Kalmykova, A. V. Volokhina and L. I. Gudim, *Vysokomolekul. Soedin.*, **14B**, 244 (1972).
26. S. P. Papkov and V. G. Kulichikhin, "Liquid-Crystalline State of Polymers" (Kimiya P. H., Moscow, 1977), p. 240 (in Russian).
27. T. Asada and S. Onogi, *Polym. Eng. Rev.*, **3**, 323 (1983).
28. S. Onogi and T. Asada, "Rheology," G. Astarita, G. Marrucci and L. Nicolais, eds. (Plenum, New York, 1980), v. 1, pp. 127-147.
29. K. Wissbrun, *Brit. Polym. J.*, **12**, 163 (1980).
30. F. N. Cogswell, *Recent Adv. Liq. Cryst. Polym. Proc. Eur. Sci. Found.*, Lingby Sept. 12-14, 1983 (London, New York, 1985), pp. 165-175.
31. F. N. Wissbrun, *Faraday Dis. Chem. Soc.*, N 79, 161 (1985).
32. R. G. Horn and M. Kleman, *Ann. Phys.*, **3**, 229 (1978).
33. V. G. Kulichikhin, N. V. Vasil'eva, V. A. Platonov, A. Ya. Malkin, and S. P. Papkov, *Vysokomolekul. Soedin.*, **21A**, 1407 (1979).
34. P. de Gennes, "The Physics of Liquid Crystals" (Clarendon Press, Oxford, 1974), p. 233.
35. M. Doi, *J. Polym. Sci., Polym. Phys. Ed.*, **19**, 229 (1981).
36. H. Enomoto, Y. Einaga, et al., *Macromolecules*, **18**, 2695 (1985).
37. S. M. Aharoni, *Polymer*, **21**, 1413 (1980).
38. T. Asada, S. Hayashida, et al., *Repts. Progr. Polym. Phys. Japan*, **23**, 145 (1980).
39. R. S. Porter and J. F. Johnson, "Rheology" (Acad. Press, New York, 1967), F. N. J. Eirich, ed., Vol. 4, Chap. 5, p. 317.
40. G. Kiss and R. S. Porter, *J. Polym. Sci., Polym. Phys. Ed.*, **18**, 361 (1980).
41. A. D. Gotsis and D. G. Baird, *Rheol. Acta*, **25**, 275 (1986).
42. S. Suto, J. L. White, et al., *Rheol. Acta*, **21**, 62 (1982).
43. T. Weng, A. Hiltner and E. Baer, *J. Mater. Sci.*, **21**, 744 (1986).
44. V. G. Kulichikhin, E. K. Borisenkova, E. M. Antipov, D. R. Tur, S. V. Vinogradova and N. A. Plate, *Vysokomolekul. Soedin.*, **29B**, 484 (1987).
45. A. K. Evseev, Yu. N. Panov and S. Ya. Frenkel', *Acta Polymerica*, **34**, 381 (1983).
46. V. G. Kulichikhin and N. P. Kruchinin, *Khim. Volokna*, N 6, 6 (1986).
47. G. A. Belinskiy and V. I. Brizitskiy, et al., *Khim. volokna*, N 4, 25 (1982).
48. V. G. Kulichikhin, N. P. Kruchinin and G. A. Belinskiy, *Khim. volokna*, N 3, 28 (1979).
49. A. A. Panfilova, V. A. Platonov, V. D. Kalmykova, A. V. Volokhina, V. G. Kulichikhin and S. P. Papkov, *Khim. volokna*, N 3, 10 (1975).
50. R. E. Christensen, *SPE J.*, **18**, 751 (1962).
51. G. A. Belinskiy, V. N. Kiya-Oglu, et al., *Khim. volokna*, N 2, 29 (1983).
52. J. C. Uyun, *AIChE J.*, **24**, 418 (1978).
53. A. L. Jarin, "Rheology of Polymer Melts and Solutions," IPM AN USSR, Prepr. N 238, Moscow, (1987).
54. Yu. P. Kozhevnikov, N. P. Kruchinin, et al., *Khim. volokna*, N 5, 34 (1981).
55. Yu. P. Kozhevnikov and A. G. Belinskaya, *Khim. volokna*, N 2, 43 (1984).
56. S. G. Efimova, A. V. Volokhina, A. I. Koretskaya, M. M. Iovleva, T. S. Sokolova and S. P. Papkov, *Vysokomolekul. Soedin.*, **14A**, 1523 (1972).
57. N. P. Kruchinin, G. A. Lavrent'ev, et al., *Khim. volokna*, N 2, 46 (1977).
58. S. P. Papkov, *Vysokomolekul. Soedin.*, **24A**, 1701 (1982).